

## Age-related Macular Degeneration

THE LIPOFUSCIN COMPONENT *N*-RETINYL-*N*-RETINYLDENE ETHANOLAMINE DETACHES PROAPOPTOTIC PROTEINS FROM MITOCHONDRIA AND INDUCES APOPTOSIS IN MAMMALIAN RETINAL PIGMENT EPITHELIAL CELLS\*

Marianne Suter‡, Charlotte Remé§, Christian Grimm§, Andreas Wenzel§, Marja Jäättelä¶, Peter Esser||, Norbert Kociok||, Marcel Leist\*\*, and Christoph Richter‡ ‡‡

From the ‡Institute of Biochemistry, Swiss Federal Institute of Technology, Universitätstr. 16, CH-8092 Zurich, Switzerland, §Laboratory for Retinal Cell Biology, Department of Ophthalmology, University Hospital Zurich, Frauenklinikstr. 24, CH-8091 Zurich, Switzerland, ¶Danish Cancer Society, Apoptosis Laboratory, Strandboulevarden 49, DK-2100 Copenhagen, Denmark, ||Eye Clinic, University of Cologne, Joseph Stelzmannstr. 9, D-50931 Cologne, Germany, and \*\*Department of Molecular Toxicology, Faculty of Biology, University of Constance, D-78457 Constance, Germany

10–20% of individuals over the age of 65 suffer from age-related macular degeneration (AMD), the leading cause of severe visual impairment in humans living in developed countries. The pathogenesis of this complex disease is poorly understood, and no efficient therapy or prevention exists to date. A precondition for AMD appears to be the accumulation of the age pigment lipofuscin in lysosomes of retinal pigment epithelial (RPE) cells. In AMD, these cells seem to die by apoptosis with subsequent death of photoreceptor cells, and light may accelerate the disease process. Intracellular factors leading to cell death are not known. Here we show that the lipophilic cation *N*-retinyl-*N*-retinylidene ethanolamine (A2E), a lipofuscin component, induces apoptosis in RPE and other cells at concentrations found in human retina. Apoptosis is accompanied by the appearance of the proapoptotic proteins cytochrome *c* and apoptosis-inducing factor in the cytoplasm and the nucleus. Biochemical examinations show that A2E specifically targets cytochrome oxidase (COX). With both isolated mitochondria and purified COX, A2E inhibits oxygen consumption synergistically with light. Inhibition is reversed by the addition of cytochrome *c* or cardiolipin, a negatively charged phospholipid that facilitates the binding of cytochrome *c* to membranes. Succinate dehydrogenase activity is not altered by A2E. We suggest that A2E can act as a proapoptotic molecule via a mitochondria-related mechanism, possibly through site-specific targeting of this cation to COX. Loss of RPE cell viability through inhibition of mitochondrial function might constitute a pivotal step toward the progressive degeneration of the central retina.

Age-related macular degeneration (AMD)<sup>1</sup> affects 10–20% of people at an age over 65 and constitutes one of the leading

causes of severe visual impairment in the elderly in industrialized nations (1). Whereas the clinical and the histopathological pictures of AMD are well known (2, 3), molecular events initiating the disease remain elusive. Major obstacles in elucidating such events are the lack of suitable animal models and the complexity of the human disease. Recent studies indicate that genetic components (4–8) and exogenous enhancing factors (9, 10) both contribute to the pathogenesis.

In the course of photoreceptor renewal, rod outer segment tips are shed and phagocytosed by the underlying cells of the retinal pigment epithelium (RPE) (11–13). It is generally believed that the accumulation of the autofluorescent age pigment lipofuscin in RPE cell phagolysosomes constitutes a predicament for the development of the disease. Lipofuscin accumulation and the formation of drusen and other deposits in the region of Bruch's membrane, which separates the pigment epithelium from the underlying choroid are considered initial steps in the pathogenesis of AMD. Drusen formation may be the result of progressive death and/or exocytosis of RPE cells in the central retina (14, 15).

Lipofuscin harbors two unusual retinoids, the lipophilic cations *N*-retinyl-*N*-retinylidene ethanolamine (A2E) and its isoform, *iso*-A2E, first isolated from the eyes of old individuals (16, 17). The molecules can be synthesized from two retinals and one ethanolamine (17), both components of photoreceptor outer segment membranes, where 11-*cis*-retinal serves as the chromophore of the visual pigment rhodopsin and phosphatidylethanolamine is an abundant membrane phospholipid.

During AMD, RPE cells may be lost by apoptosis as evidenced with human autopsy eyes (18). Apoptosis is a form of cell death that, in addition to its physiological importance in tissue development and homeostasis (19), plays a major role in diseases such as cancer, acquired immune deficiency syndrome, autoimmune diseases, and tissue degeneration (for a review, see Ref. 20). Mitochondria are important control centers of apoptosis (21, 22). When they are destabilized, for example by oxidative stress, they release apoptosis-inducing proteins. One is cytochrome *c*, which in the cytoplasm often but not always (23) activates caspases, apoptosis-specific proteases. Another protein is apoptosis-inducing factor (AIF), which induces nuclear apoptosis independently of caspase activation (24, 25). Present knowledge suggests that mitochondria function as cellular sensors of stress into which different apoptosis

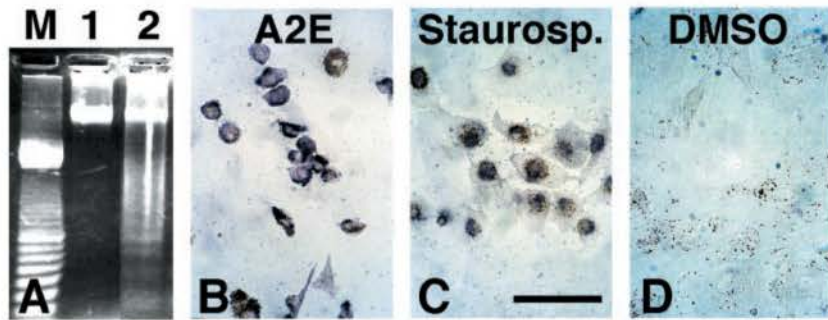
damine ethylester; HPLC, high pressure liquid chromatography; TUNEL, terminal deoxynucleotidyl transferase-mediated dUTP nick end labeling .

\* The costs of publication of this article were defrayed in part by the payment of page charges. This article must therefore be hereby marked "advertisement" in accordance with 18 U.S.C. Section 1734 solely to indicate this fact.

‡‡ To whom correspondence should be addressed: Institute of Biochemistry, Swiss Federal Institute of Technology, Universitätstr. 16, CH-8092 Zurich, Switzerland. Tel.: 41-1-6323021 or -6323136; Fax: 41-1-6321121; E-mail: richter@bc.biol.ethz.ch.

<sup>1</sup> The abbreviations used are: AMD, age-related macular degeneration; AIF, apoptosis-inducing factor; A2E, *N*-retinyl-*N*-retinylidene ethanolamine (2-[2,6-dimethyl-8-(2,6,6-trimethyl-1-cyclohexen-1-yl)-1E,3E,5E,7E-octatetraenyl]-1-(2-hydroxyethyl)-4-[4-methyl-6-(2,6,6-trimethyl-1-cyclohexen-1-yl)-1E,3E,5E-hexatrienyl]-pyridinium); CGC, cerebellar granule cells; COX, cytochrome oxidase; RPE, retinal pigment epithelium; MTT, 3-(4,5-dimethylthiazole-2-yl)-2,5-diphenyltetrasodium bromide; TMRE, tetramethylrh-

**FIG. 1. A2E induces apoptosis in retinal pigment epithelial cells.** A, cultured retinal pigment epithelium cells were exposed to 50  $\mu\text{M}$  A2E in 0.5%  $\text{Me}_2\text{SO}$  (lane 2) or to solvent alone (lane 1). DNA was extracted after 24 h and analyzed by agarose gel electrophoresis. M, 100-base pair DNA ladder as marker. B–D, TUNEL staining of cells exposed for 24 h to 25  $\mu\text{M}$  A2E (B), 0.5  $\mu\text{M}$  staurosporine (C), or 0.5%  $\text{Me}_2\text{SO}$  (DMSO) (D). Scale bar, 100  $\mu\text{m}$ .



induction pathways converge and that mitochondria act as central executioners of apoptosis (26).

We show here that A2E induces apoptosis in cultures of various mammalian cell types, including RPE cells. A2E-induced apoptosis is preceded by a decline in mitochondrial activity and is accompanied by translocation of cytochrome *c* and AIF into the cytoplasm and nucleus. Biochemical experiments suggest that A2E targets directly the function of COX, whereas respiratory chain activity upstream of cytochrome *c* is not affected by A2E. We propose that A2E can induce apoptosis by mobilizing cytochrome *c* and AIF from mitochondria. Our findings give insight into the molecular mechanism underlying A2E's cytotoxicity and suggest strategies to retard or overcome AMD.

#### EXPERIMENTAL PROCEDURES

**Animals**—8-Day-old specific pathogen free BALB/c mice were obtained from the Animal Unit of the University of Constance, and female Wistar rats were from the Animal Unit of the Institute of Biochemistry (Swiss Federal Institute of Technology, Zurich). All experiments were performed in accordance with international guidelines to minimize pain and discomfort (National Institutes of Health guidelines and European Community Council Directive 86/609/EEC) and conformed to the ARVO statement for care and use of animals in research.

**Cell Culture**—RPE cells were prepared from porcine eyes obtained from a local slaughterhouse essentially as described previously (27). The purity of the culture was verified by immunohistochemical staining with anti-cytokeratin antibodies (Sigma c-2931). Experiments were performed with passage 1–2 RPE cells that were maintained in Dulbecco's modified Eagle's medium containing 10% fetal calf serum, 50  $\mu\text{g}/\text{ml}$  gentamicin, and 2.5  $\mu\text{g}/\text{ml}$  amphotericin.

Murine cerebellar granule cells (CGC) were isolated from 8-day-old BALB/c mice and cultured as described (28). Contamination with non-neuronal cells ( $\beta$ -III-tubulin-negative) was <5%. Dissociated neurons were plated on 100  $\mu\text{g}/\text{ml}$  (250  $\mu\text{g}/\text{ml}$  for glass surfaces) poly-L-lysine (> 300 kDa)-coated dishes at a density of about  $0.25 \times 10^6$  cells/cm<sup>2</sup> (800,000 cells/ml; 500  $\mu\text{l}/\text{well}$ , 24-well plate) and cultured in Eagle's basal medium (Life Technologies, Inc.) supplemented with 10% heat-inactivated fetal calf serum, 20 mM KCl, 2 mM L-glutamine plus penicillin/streptomycin, and cytosine arabinoside (10  $\mu\text{M}$ ; added 48 h after plating). CGC were used without further medium changes after 5 days in culture. The cells were exposed to A2E in their original medium in the presence of 2  $\mu\text{M}$  (+)-5-methyl-10,11-dihydro-5H-dibenzo[a,d]cyclohepten-5,10-imine (MK801; Biotrend Chemikalien GmbH) and 2 mM  $\text{Mg}^{2+}$  to prevent N-methyl-D-aspartate receptor activation and excitotoxicity (29, 30).

**Viability Assays**—Apoptosis and secondary lysis were routinely quantified by double staining of neuronal cultures with 1  $\mu\text{g}/\text{ml}$  H-33342 (membrane-permeant, blue fluorescent chromatin stain; Molecular Probes, Inc., Eugene, OR) and 0.5  $\mu\text{M}$  SYTOX (non-membrane-permeant, green fluorescent chromatin stain; Molecular Probes) as described previously (31, 32). Apoptotic cells were characterized by scoring typically condensed nuclei. About 200–300 cells were counted in two or three different culture wells, and experiments were repeated with at least three different preparations. In addition, mitochondrial activity was quantified by the reduction of 3-(4,5-dimethylthiazole-2-yl)-2,5-diphenyltetrazolium bromide (MTT) (incubation for 60 min with 0.5 mg MTT/ml).

**Immunocytochemistry**—CGC were grown on glass-bottomed culture

dishes, fixed after the experiment with 4% paraformaldehyde, and permeabilized with 0.1% Triton X-100 (for cytochrome *c*) or 0.1% SDS (for AIF). Staining of cytochrome *c* (anti-cytochrome *c* antibody; clone 6H2.B4, Pharmingen, Hamburg, Germany) was performed as described (33, 34). Rabbit anti-AIF serum (24) was used at a dilution of 1:500. Alexa<sup>TM</sup>-568 coupled anti-mouse IgG antibody (1:300; Molecular Probes) served as secondary antibody. CGC were embedded in phosphate-buffered saline containing 50% glycerol and 0.5  $\mu\text{g}/\text{ml}$  H-33342 and imaged by confocal microscopy (TCS-4D UV/VIS confocal scanning system; Leica AG, Benzheim, and Leica Lasertechnik, Heidelberg, Germany). A2E shows a strong green and red fluorescence when excited at 488 or 568 nm. The red fluorescence is very photolabile and can be eliminated by short illumination with a 50-watt lamp. Thereafter A2E fluorescence in the green channel was easily distinguished from the fluorescence of red-emitting fluorophores used for co-staining.

**Mitochondrial Membrane Potential**—Mitochondrial membrane potential in CGC was monitored as described (23, 29) after loading cells with 5 nM tetramethylrhodamine ethylester (TMRE; Molecular Probes) on a coverslip-bottomed cell culture dish. The images were obtained with a confocal microscope (Leica TCS-4D; Leica, Heidelberg, Germany) and a  $\times 63$ , NA 1.32 lens. For dissipation of the membrane potential, carbonylcyanide-3-chlorophenylhydrazone was added to the cultures. The decay of TMRE fluorescence (excitation, 568 nm; emission, > 586 nm) and of A2E fluorescence (excitation, 488 nm; emission, > 515 nm) was monitored individually in control experiments or simultaneously with A2E fluorescence (A2E emission filter set to  $520 \pm 10$  nm).

**Synthesis, Purification, and HPLC Analysis of A2E and iso-A2E**—A2E and iso-A2E were synthesized from all-trans-retinal and ethanolamine as described (17) and purified chromatographically on silica gel 60 thin layer chromatography plates using the primary developing system (35). A2E and iso-A2E, the former being the faster moving band, were detected on the plates by their fluorescence upon illumination with 366-nm light. The material containing A2E and iso-A2E was scraped off, eluted with chloroform/methanol/water (30/25/4), dried, and rechromatographed. Stock solutions of A2E and iso-A2E were stored in  $\text{Me}_2\text{SO}$  at  $-20^\circ\text{C}$  in the dark. Total A2E diluted into methanol was quantified using a molar extinction coefficient of 36,900 at 439 nm (17). For HPLC, total A2E was loaded onto a reversed phase column (Nucleosil 100–5 C18;  $150 \times 4.6$  mm; Macherey-Nagel, Oensingen, Switzerland) and eluted with a gradient of methanol (plus 0.1% trifluoroacetic acid) in water (86–100% in 20 min). A2E and iso-A2E were detected at 436 nm with a peak maximum at 16 and 19 min, respectively.

**Photoisomerization of A2E and iso-A2E**—Photoisomerization was induced by illuminating purified A2E or iso-A2E with white light (70 watts, at 14-cm distance). The extent of isomerization was analyzed by HPLC analysis (see above). The isomers reached equilibrium in about 10 min.

**Cytotoxicity of A2E and Apoptosis Assays**—A2E was diluted into the RPE cell culture medium to a concentration of 25  $\mu\text{M}$  A2E and 0.5%  $\text{Me}_2\text{SO}$ . Control incubations were done with 0.5%  $\text{Me}_2\text{SO}$  in the absence of A2E as negative control and with 0.5  $\mu\text{M}$  staurosporine as positive control. Incubation was at  $37^\circ\text{C}$  with 5%  $\text{CO}_2$  for 24 h in darkness. For TUNEL staining (TUNEL assay; Roche Molecular Biochemicals), formaldehyde-fixed cells were equilibrated in 30 mM Tris, 140 mM sodium cacodylate, pH 7.2, treated with terminal transferase (0.25 units/ $\mu\text{l}$ ) and biotin-dUTP (20  $\mu\text{M}$ ) in the above buffer containing 1 mM cobalt chloride for 60–90 min at  $37^\circ\text{C}$ , washed in 300 mM NaCl, 30 mM sodium citrate, for 15 min, rinsed twice in  $\text{H}_2\text{O}$ , blocked for 10 min with 2% bovine serum albumin in phosphate-buffered saline, treated with streptavidin-alkaline phosphatase diluted 1:500 in 100 mM Tris, 50 mM NaCl, pH 7.5, rinsed five times in  $\text{H}_2\text{O}$ , and developed using nitro blue

tetrazolium chloride and 5-bromo-4-chloro-3-indolyl phosphate as a substrate. The slides were not counterstained.

**DNA Fragmentation Analysis**—After incubation with A2E (50  $\mu\text{M}$ ; 0.5% Me<sub>2</sub>SO; 16 h; 5% CO<sub>2</sub>; 37 °C; darkness), cells were scraped from the plates, washed once in phosphate-buffered saline, and resuspended in 1 ml of 10 mM Tris (pH 8), 10 mM EDTA, and 10 mM NaCl. SDS was added to a final concentration of 0.5%, and proteins were digested with proteinase K (0.2 mg/ml) at 37 °C for 5 h. Fresh proteinase K was added (0.2 mg/ml), and incubation was continued for 4 h at 50 °C. The mixture was extracted once with phenol/chloroform/isoamylalcohol (25:24:1) and twice with chloroform/isoamylalcohol (24:1). NaCl (final concentration 300 mM) and ethanol (2.5 volumes) were added, and DNA was precipitated overnight at -20 °C. After centrifugation for 10 min at 4000  $\times g$  (4 °C), DNA was washed once with 70% ethanol and air-dried for 1 h at room temperature. 100  $\mu\text{l}$  of 10 mM Tris, pH 8, 1 mM EDTA, were added, and DNA was allowed to rehydrate for 2 days at 4 °C. RNA was digested by incubation at 37 °C for 1 h with 20  $\mu\text{g}$  of RNase A. DNA concentration was determined by A<sub>260</sub> reading. 15  $\mu\text{g}$  of total DNA were analyzed by electrophoresis on a 1.5% agarose gel and stained with SybrGreen (Molecular Probes).

**Isolation of Mitochondria and Cytochrome Oxidase**—Liver mitochondria were obtained from overnight-starved rats weighing 200 g by differential centrifugation (36). COX was isolated from rat liver as described (37).

**Oxygen Consumption Measurements**—Oxygen consumption was measured at 28 °C with a Clark-type oxygen electrode (YSI, Inc., Yellow Springs, OH) under continuous stirring. Mitochondria were diluted to 1 mg of mitochondrial protein/ml in a buffer containing 300 mM sucrose, 5 mM HEPES, pH 7.4, 0.5 mM EGTA, and 0.5 mg of fatty acid-free bovine serum albumin/ml. A2E was added to the mitochondrial suspension before rotenone (5  $\mu\text{M}$ ) and succinate (0.4–1.2 mM). The reaction time was normally 4 min or as indicated. Cytochrome *c* (1  $\mu\text{M}$ ) or cardiolipin (1  $\mu\text{g}/\text{ml}$ ) was added as indicated. COX (263  $\mu\text{g}/\text{ml}$ ) assays were performed in 40 mM phosphate buffer, pH 7.0, and 50  $\mu\text{M}$  EDTA with 1 mM ascorbate and 0.4 mM tetramethyl-*p*-phenylenediamine.

## RESULTS

**A2E Induces Apoptosis in Retinal Pigment Epithelial Cells**—A2E, a component of lipofuscin in the RPE (16, 38) affects lysosomal function (39), inhibits growth of human RPE cells *in vitro* (40, 41), and mediates blue light-induced apoptosis to RPE cells (42). To investigate the molecular details of A2E toxicity, we isolated and cultured pig RPE cells and exposed them to increasing concentrations of A2E. Application of as little as 25  $\mu\text{M}$  A2E, which results in an intracellular content of A2E found in human eyes (40), induces apoptosis in PRE cells within 24 h as evidenced by the internucleosomal DNA fragmentation of genomic DNA (Fig. 1A) and positive TUNEL staining (Fig. 1B). The latter was comparable with the staining caused by staurosporine, a known apoptosis-inducing agent (Fig. 1C), and was not detected in cells exposed to solvent alone (Fig. 1D).

**A2E Accumulates in Mitochondria and Induces Release of Proapoptotic Mitochondrial Proteins**—Mitochondria participate in the execution of apoptosis induced by many agents, including lipophilic cations (29) and can release proapoptotic proteins. This is often but not always followed by activation of

proteases known as caspases. Because we suspected an involvement of mitochondria in cell death induced by the lipophilic cation A2E, we also investigated cerebellar granule cells (CGC), in which mitochondria abound. Significant apoptotic death was induced in these cells at A2E concentrations of >10  $\mu\text{M}$ . Interestingly, already lower A2E concentrations decreased mitochondrial function as measured by the MTT assay (Fig. 2) or a decrease in TMRE fluorescence (not shown). The decline in mitochondrial activity precedes the death of CGC (Fig. 2). These cells accumulate A2E in mitochondria as shown by comparison of the localization of A2E with the mitochondrial marker TMRE (Fig. 3A). We found that after deenergization of mitochondria in CGC A2E is for presently unknown reasons retained much longer than TMRE in the organelles (Fig. 3B), an observation confirmed with isolated rat liver mitochondria.<sup>2</sup> The cells release in response to A2E the proapoptotic proteins cytochrome *c* (Fig. 4, A–F) and AIF (Fig. 4, G–M) from mitochondria into the cytoplasm and nucleus. The two other cell types tested, the neuroblastoma lines CHP-100 and SH-SY5Y, also underwent apoptosis when exposed to A2E in a similar concentration range (data not shown). In none of the cell types investigated was death induced by A2E apparently related to caspase activation, since death was not preventable by 100  $\mu\text{M}$  benzoyloxycarbonyl-Val-Ala-Asp-fluoromethyl ketone or other established caspase inhibitors (data not shown). Similarly, A2E treatment did not activate caspase-3 in cultured RPE cells (data not shown).

**A2E Inhibits Respiration of Isolated Mitochondria and Cytochrome Oxidase**—A2E is a lipophilic cation, and energized mi-

<sup>2</sup> C. Richter, unpublished result.

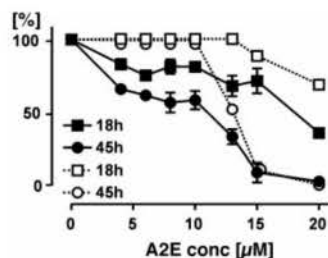


**FIG. 2. A2E decreases mitochondrial activity and causes loss of cell viability.** CGC were incubated in medium containing A2E concentrations as indicated. After 18 and 45 h, the capacity of the cell population to reduce MTT (mitochondrial activity) was determined (closed symbols). Data are standardized to untreated control cells as 100% reference value. In parallel cultures, cell viability was determined by staining with the chromatin dyes H-333342 and SYTOX. The percentage of cells with intact plasma membrane and noncondensed chromatin (open symbols) was determined. Data represent means  $\pm$  S.D. of three independent experiments.

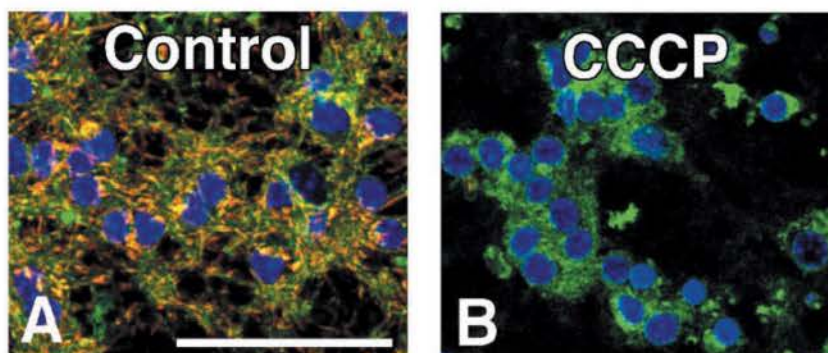


**FIG. 3. A2E is localized in mitochondria.** CGC cultures were exposed to A2E (20  $\mu\text{M}$ ) for 6 h. Solvent (A) or carbonyl-cyanide-3-chlorophenylhydrazone (CCCP, 100  $\mu\text{M}$ ) (B) was added, and live neurons were stained with TMRE and H-333342 and imaged by multichannel confocal microscopy. A2E fluorescence is represented in green, TMRE in red, and chromatin structure in blue. Co-localization of A2E and TMRE appears as yellow (artificial color fusions). Scale bar, 50  $\mu\text{m}$ .

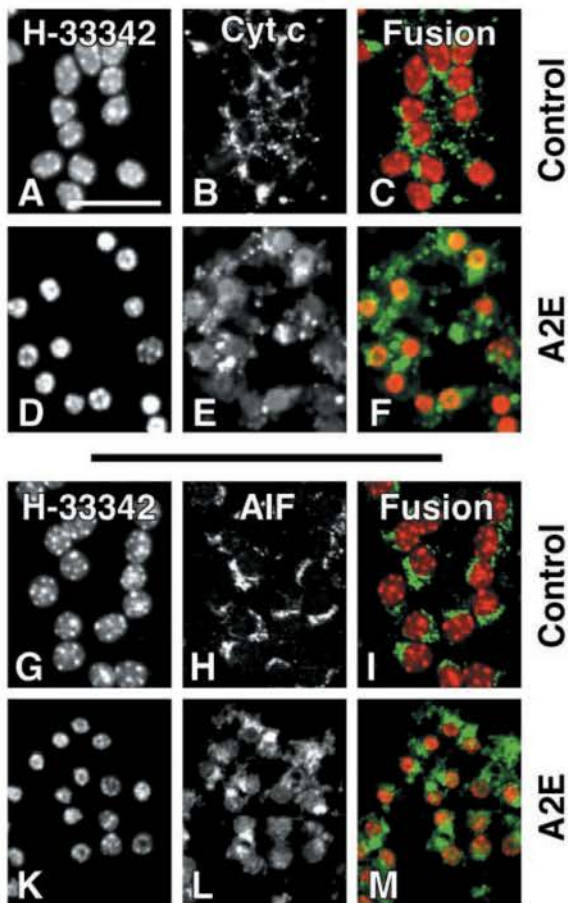


**FIG. 4. A2E triggers release of cytochrome *c* and of apoptosis-inducing factor.** A–F, CGC cultures were exposed to 20  $\mu$ M A2E (D–F) or solvent (A–C) for 20 h, fixed, stained for chromatin structure (H-333342, red; A and D) and cytochrome *c* (green; B and E), and imaged by confocal microscopy. Optical sections were obtained at the level of the neuronal somata, where mitochondria (B) lie in a close circle around the nucleus. A2E leads to the appearance of cytochrome *c* in the cytosol and the nucleus as evidenced by the fusion image (yellow; F). G–M, CGC cultures were exposed to 20  $\mu$ M A2E (K–M) or solvent control (G–I), fixed after 24 h, stained for chromatin structure (H-333342, red; G and K) and apoptosis-inducing factor (green; H and L), and imaged simultaneously by confocal microscopy (I and M). A2E leads to the appearance of AIF in the cytosol and the nucleus as evidenced by the fusion image (yellow; M). Scale bar, 25  $\mu$ m.

mitochondria avidly accumulate such ions via their membrane potential. To gain insight into the mechanism by which A2E induces apoptosis, we investigated the response of isolated mitochondria and COX to A2E. Fig. 5 shows that oxygen consumption by mitochondria respiring on succinate is suppressed by A2E in a dose-dependent manner (Fig. 5A), A2E being more potent in the light than in the dark (Fig. 5, B and C). In contrast to A2E, *iso*-A2E inhibits respiration only marginally (Fig. 5B), most of the observed inhibition being attributable to the conversion by light of *iso*-A2E to A2E. The A2E-induced inhibition is apparently due to detachment of cytochrome *c* from mitochondria, because inhibition can be overcome by added cytochrome *c* or cardiolipin (Fig. 5, C and D). When cardiolipin is added before A2E, the latter is slightly less effective than when the order of addition is reversed (Fig. 5D, trace *a* versus trace *b*). Although the difference is not very pronounced, it was observed in every experiment ( $n = 4$ ). Succinate-

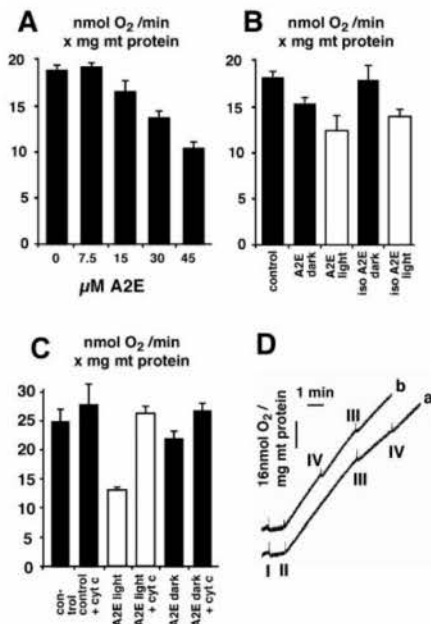


**FIG. 5. A2E inhibits mitochondrial respiration.** Oxygen consumption of mitochondria isolated from rat liver was measured in the absence and presence of A2E in a Clarke-type electrode in the dark (aluminum foil-wrapped) or under light (70-watt tungsten lamp, 40-cm distance). A, concentration dependence of A2E inhibition in the dark. B, comparison of 10  $\mu$ M HPLC-purified A2E and *iso*-A2E (content  $89.2 \pm 1.4$  or  $59.2 \pm 7.8\%$ , respectively). C, reversal of A2E (15  $\mu$ M) inhibition by cytochrome *c* (1  $\mu$ M). D, reversal of A2E (15  $\mu$ M) inhibition by cardiolipin (1  $\mu$ g/ml). The following additions were made: rotenone (5  $\mu$ M) (I); succinate (0.5 mM) (II); A2E (15  $\mu$ M) (III); cardiolipin (1  $\mu$ g/ml) (IV). Note that the order of addition of A2E and cardiolipin is reversed in traces *a* and *b*; representative recordings are shown. The columns in A–C represent mean values  $\pm$  S.D. of four independent experiments.

nate-ferricyanide oxidoreductase activity, which reflects electron flow from succinate via its dehydrogenase to cytochrome  $bc_1$ , was not affected by A2E, nor was the reduction of cytochrome *c* by the artificial electron donor dithionite (data not shown).

Cardiolipin facilitates the binding of cytochrome *c* to COX-containing membranes (43). The above results strongly suggest that A2E inhibits mitochondrial respiration because it prevents cytochrome *c* binding to the inner mitochondrial membrane and thereby interrupts electron flow between cytochrome  $bc_1$  and COX. To substantiate this, we measured oxygen consumption of isolated COX. This is possible when electrons are provided by ascorbate and mediated to cytochrome *c* by the dye tetramethyl-*p*-phenylenediamine. Fig. 6A shows that also in this well defined system, comprising besides the electron donor/mediator only two proteins and COX-bound cardiolipin, A2E inhibits oxygen consumption dose-dependently. Again, inhibition is counteracted by cardiolipin addition (Fig. 6B, trace *a* versus trace *b*). When cardiolipin is added before A2E in this system, A2E is totally ineffective (Fig. 6, B, trace *c* versus trace *d*). As with mitochondria, *iso*-A2E inhibited COX only marginally (data not shown).

#### DISCUSSION

Loss of pigment epithelial cells in the retina may result in the so-called geographic atrophy, which is by far the most frequent form of AMD. To date, no cure or prevention of this disease, which affects a large number of elderly people, is available. A better understanding of the molecular details of AMD's pathogenesis promises to provide rationales to success-

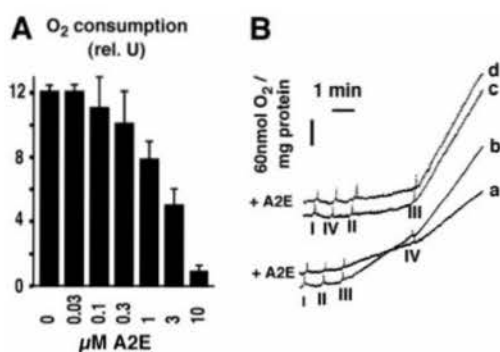


FIG. 6. A2E inhibits oxygen consumption by cytochrome oxidase. Oxygen consumption of cytochrome oxidase isolated from rat liver was measured in the absence and presence of A2E in a Clarke-type electrode. A, the columns represent mean values  $\pm$  S.D. of four independent experiments. B, reversal of A2E (3  $\mu$ M) inhibition by cardiolipin (1  $\mu$ g/ml). The following additions were made: ascorbate/TMPD (I); COX (II); cytochrome *c* (III); cardiolipin (IV). Representative recordings are shown. For experimental details, see "Experimental Procedures."

fully retard the onset of the disease or even prevent it. Here we show by several complementary experimental approaches that the cationic A2E accumulates in mitochondria, inhibits mitochondrial function, detaches proapoptotic proteins from mitochondria and may thereby induce apoptosis.

A2E and its isomer *iso*-A2E have been isolated from the eyes of elderly humans (17, 44) and rats (see below), but it is presently unclear where and how these molecules are formed. *In vitro*, A2E and *iso*-A2E are readily synthesized by mixing all-*trans*-retinal with ethanolamine at slightly acidic pH (17). *In vivo*, when light strikes the visual pigment rhodopsin, the chromophore all-*trans*-retinal is liberated from the photoreceptor outer segment membranes, reduced, and transported into the RPE. Additionally, packets of photoreceptor discs are rhythmically shed and phagocytosed by RPE cells (12). The last steps of A2E formation were suggested to occur in RPE phagolysosomes due to the requirement of oxidizing and acidic conditions (44) and shown to result from the reaction of all-*trans*-retinal molecules with a phosphatidylethanolamine molecule, followed by hydrolysis of the adduct (44). A2E was also detected in lysosomes of cells exposed in culture to the free compound or to A2E coupled to low density lipoprotein particles (40, 45). A2E inhibits hydrolytic activities in lysosomes (14, 39) and mediates blue light-induced damage to RPE cells (42).

Energized mitochondria establish across their inner membrane an electric potential, negative charge inside, which drives sufficiently lipophilic cations nonspecifically into the organelles (46). We therefore suspected that the lipophilic cations A2E and *iso*-A2E accumulate in mitochondria. Our confocal microscopic study indeed revealed the predominant presence of A2E in CGC mitochondria. The presence of A2E in lysosomes but not in mitochondria reported by others (39, 40), and the mitochondrial localization found in our study may suggest that after damaging lysosomes A2E can be released and subsequently taken up by mitochondria. Alternatively, A2E may initially accumulate in and be retained by mitochondria, which when damaged may be engulfed by lysosomes. In contrast to these presumably physiological intracellular steps of A2E distribution pathogenetic steps leading to cell death may be mainly due to overloading of mitochondria with the lipophilic cation.

A2E and *iso*-A2E are detergent-like wedge-shaped molecules with slightly different dimensions. Their biological properties have not been studied in detail, and it also remained to be elucidated whether both isomers are relevant in the disease

process. We find that A2E dose-dependently induces apoptosis in mammalian RPE cells, approximately 50% killing of the cultured cells being achieved with 25  $\mu$ M A2E. How may this relate to the *in vivo* situation? From one eye of elderly humans on average about 830 pmol were isolated (17). Assuming that in the eye A2E is present exclusively in RPE cells and evenly distributed, a concentration of about 15  $\mu$ M A2E in such cells of elderly humans can be calculated. The age-related increase in human eyes is corroborated by an age-dependent accumulation of A2E in rat eyes. Thus, we detected on average about 4 pmol of A2E in the eyes of rats weighing 200 g and 42 pmol of A2E in the eyes of rats weighing about 350 g.

Apoptosis induced by A2E is preceded by a decline of mitochondrial activity and is accompanied by the appearance of cytochrome *c* and AIF in the cytosol and nucleus, respectively. The detachment of cytochrome *c* from the inner mitochondrial membrane has at least two important consequences for mitochondria. First, they experience oxidative stress because the reduction of the respiratory chain members upstream of the cytochrome *c* binding sites results in enhanced superoxide formation (47); second, when electron flow is interrupted, mitochondrial ATP synthesis is impaired. Both events are highly relevant for apoptosis because oxidative stress and decreased energy levels further weaken mitochondria, cause leakiness of their inner membrane, and favor release of proapoptotic proteins from mitochondria (21, 48). AIF, a novel pro-apoptotic protein, is strictly confined to mitochondria, and translocates to the nucleus upon induction of apoptosis by various stimuli (25). AIF translocation is correlated with large scale DNA fragmentation and is probably responsible for apoptosis morphology in the absence of caspases (24, 25).

At the cellular level, release of cytochrome *c* often but not always results in the activation of the caspase cascade. In cells with a defect in ATP generation activation of caspases can be entirely prevented despite high cytosolic cytochrome *c* concentrations (23, 30, 32). This may explain the lack of inhibition of A2E-induced cell death by the pancaspase inhibitor benzyloxy-carbonyl-Val-Ala-Asp-fluoromethyl ketone. Thus, caspases may play at most only a minor role in A2E-induced apoptosis. There are *in vitro* precedents for apoptosis independent of caspase activation in the retina (49) or tumor cells (50).

To gain additional insight into the mechanism(s) by which A2E might induce apoptosis, we studied its action on isolated mitochondria and COX. We find inhibition by A2E but not by *iso*-A2E of mitochondrial succinate-supported oxygen consumption and relief of the inhibition by added cytochrome *c* or cardiolipin, a unique phospholipid almost exclusively located in the inner mitochondrial membrane, where it supports oxidative phosphorylation (51–53). The restoration of respiratory activity may be due to a direct interaction of A2E and cardiolipin at the level of COX or to binding of the anionic cardiolipin to the cationic A2E in solution. As to the latter, we did not detect by UV-visible spectroscopy complex formation between the two compounds (data not shown). Electron flow from succinate dehydrogenase to complex III of the respiratory chain, however, is not affected by A2E, as shown by ferricyanide reduction measurements. These findings indicate that in mitochondria A2E impairs specifically the interaction between cytochrome *c* and COX, a result corroborated by the data obtained with the isolated enzyme complex. *iso*-A2E causes only minor inhibition of respiration by mitochondria or isolated COX, most or all of it being attributable to the conversion of *iso*-A2E to A2E. This further underlines the specificity of A2E's action and argues against a simple detergent-like effect of the amphiphilic compound.

So far, no efficient AMD therapy or prevention exists. Caro-

tenoids and antioxidants (54), limiting exposure to light, or targeting of the precursors of A2E (44) may be useful. Our findings suggest several other promising strategies. One is supplementation with cardiolipin to facilitate retention of cytochrome *c* in mitochondria, because the mitochondrial cardiolipin content and function decrease in humans progressively with age to about 60% of the value found in children (55, 56). Another possible strategy is the prevention of A2E formation by, for example, outcompeting ethanolamine with a secondary amine or outcompeting retinal with another aldehyde. Since the level of retinal is decreased by retinal dehydrogenase, stimulation of this enzyme may also be useful to counteract AMD.

**Acknowledgment**—We thank Dr. Paolo Gazzotti (Institute of Biochemistry, Swiss Federal Institute of Technology, Zurich) for kindly providing rat liver COX and Heike Naumann for expert technical assistance.

## REFERENCES

- Klein, R., Klein, B. E., and Linton, K. L. (1992) *Ophthalmology* **99**, 933–943
- Bressler, N. M., Bressler, S. B., and Fine, S. L. (1988) *Surv. Ophthalmol.* **32**, 375–413
- Zarbin, M. A. (1998) *Eur. J. Ophthalmol.* **8**, 199–206
- Allikmets, R., Shroyer, N. F., Singh, N., Seddon, J. M., Lewis, R. A., Bernstein, P. S., Peiffer, A., Zabriskie, N. A., Li, Y., Hutchinson, A., Dean, M., Lupski, J. R., and Leppert, M. (1997) *Science* **277**, 1805–1807
- Allikmets, R. (1999) *Eur. J. Ophthalmol.* **9**, 255–265
- Gorin, M. B., Breitner, J. C., De Jong, P. T., Hageman, G. S., Klaver, C. C., Kuehn, M. H., and Seddon, J. M. (1999) *Mol. Vis.* **5**, 29
- Silvestri, G. (1997) *Mol. Med. Today* **3**, 84–91
- Weng, J., Mata, N. L., Azarian, S. M., Tzekov, R. T., Birch, D. G., and Travis, G. H. (1999) *Cell* **98**, 13–23
- Cruickshanks, K. J., Klein, R., and Klein, B. E. (1993) *Arch. Ophthalmol.* **111**, 514–518
- Leibowitz, H. M., Krueger, D. E., Maunder, L. R., Milton, R. C., Kini, M. M., Kahn, H. A., Nickerson, R. J., Pool, J., Colton, T. L., Ganley, J. P., Loewenstein, J. I., and Dawber, T. R. (1980) *Surv. Ophthalmol.* **24**, (suppl.), 335–610
- Young, R. W., and Bok, D. (1969) *J. Cell Biol.* **42**, 392–403
- Young, R. W. (1976) *Invest. Ophthalmol. Vis. Sci.* **15**, 700–725
- Feeney, L. (1978) *Invest. Ophthalmol. Vis. Sci.* **17**, 583–600
- Eldred, G. E. (1995) *Gerontology* **41**, (Suppl. 2), 15–28
- Ishibashi, T., Patterson, R., Ohnishi, Y., Inomata, H., and Ryan, S. J. (1986) *Am. J. Ophthalmol.* **101**, 342–353
- Eldred, G. E., and Lasky, M. R. (1993) *Nature* **361**, 724–726
- Parish, C. A., Hashimoto, M., Nakanishi, K., Dillon, J., and Sparrow, J. (1998) *Proc. Natl. Acad. Sci. U. S. A.* **95**, 14609–14613
- Xu, G. Z., Li, W. W., and Tso, M. O. (1996) *Trans. Am. Ophthalmol. Soc.* **94**, 411–430
- Kerr, J. F., Wyllie, A. H., and Currie, A. R. (1972) *Br. J. Cancer* **26**, 239–257
- Thompson, C. B. (1995) *Science* **267**, 1456–1462
- Kroemer, G., and Reed, J. C. (2000) *Nat. Med.* **6**, 513–519
- Wallace, D. C. (1999) *Science* **283**, 1482–1488
- Leist, M., Single, B., Naumann, H., Fava, E., Simon, B., Kuhnle, S., and Nicotera, P. (1999) *Exp. Cell Res.* **249**, 396–403
- Susin, S. A., Lorenzo, H. K., Zamzami, N., Marzo, I., Snow, B. E., Brothers, G. M., Mangion, J., Jacotot, E., Costantini, P., Loeffler, M., Larochette, N., Goodlett, D. R., Aebbersold, R., Siderovski, D. P., Penninger, J. M., and Kroemer, G. (1999) *Nature* **397**, 441–446
- Daugas, E., Susin, S. A., Zamzami, N., Ferri, K. F., Irinopoulou, T., Larochette, N., Prevost, M. C., Leber, B., Andrews, D., Penninger, J., and Kroemer, G. (2000) *FASEB J.* **14**, 729–739
- Susin, S. A., Lorenzo, H. K., Zamzami, N., Marzo, I., Brenner, C., Larochette, N., Prevost, M. C., Alzari, P. M., and Kroemer, G. (1999) *J. Exp. Med.* **189**, 381–394
- Esser, P., Grisanti, S., Kociok, N., Abts, H., Hueber, A., Unfried, K., Heimann, K., and Weller, M. (1997) *Invest. Ophthalmol. Vis. Sci.* **38**, 2852–2856
- Schousboe, A., Meier, E., Dreijer, J., and Hertz, L. (1989) in *A Dissection and Tissue Culture Manual of the Nervous System* (Sahar, A., de Vellis, J., Vernadakis, A., and Haber, B., eds) pp. 203–206, A. R. Liss, New York
- Leist, M., Volbracht, C., Fava, E., and Nicotera, P. (1998) *Mol. Pharmacol.* **54**, 789–801
- Volbracht, C., Leist, M., and Nicotera, P. (1999) *Mol. Med.* **5**, 477–489
- Leist, M., Fava, E., Montecucco, C., and Nicotera, P. (1997) *Eur. J. Neurosci.* **9**, 1488–1498
- Leist, M., Single, B., Castoldi, A. F., Kuhnle, S., and Nicotera, P. (1997) *J. Exp. Med.* **185**, 1481–1486
- Single, B., Leist, M., and Nicotera, P. (1998) *Cell Death Differ.* **5**, 1001–1003
- Latta, M., Kunstle, G., Leist, M., and Wendel, A. (2000) *J. Exp. Med.* **191**, 1975–1986
- Eldred, G. E., and Katz, M. L. (1988) *Exp. Eye Res.* **47**, 71–86
- Schlegel, J., Schweizer, M., and Richter, C. (1992) *Biochem. J.* **285**, 65–69
- Aldez, I. Z., and Cascarano, J. (1977) *J. Bioenerg. Biomembr.* **9**, 237–253
- Reinboth, J. J., Gautschi, K., Munz, K., Eldred, G. E., and Reme, C. E. (1997) *Exp. Eye Res.* **65**, 639–643
- Holz, F. G., Schutt, F., Kopitz, J., Eldred, G. E., Kruse, F. E., Volker, H. E., and Cantz, M. (1999) *Invest. Ophthalmol. Vis. Sci.* **40**, 737–743
- Sparrow, J. R., Parish, C. A., Hashimoto, M., and Nakanishi, K. (1999) *Invest. Ophthalmol. Vis. Sci.* **40**, 2988–2995
- Cubeddu, R., Taroni, P., Hu, D. N., Sakai, N., Nakanishi, K., and Roberts, J. E. (1999) *Photochem. Photobiol.* **70**, 172–175
- Sparrow, J. R., Nakanishi, K., and Parish, C. A. (2000) *Invest. Ophthalmol. Vis. Sci.* **41**, 1981–1989
- Salamon, Z., and Tollin, G. (1996) *Biophys. J.* **71**, 858–867
- Mata, N. L., Weng, J., and Travis, G. H. (2000) *Proc. Natl. Acad. Sci. U. S. A.* **97**, 7154–7159
- Holz, F. G., Schutt, F., Kopitz, J., and Volker, H. E. (1999) *Ophthalmologie* **96**, 781–785
- Chen, L. B. (1988) *Annu. Rev. Cell Biol.* **4**, 155–181
- Cai, J., and Jones, D. P. (1998) *J. Biol. Chem.* **273**, 11401–11404
- Richter, C., Schweizer, M., Cossarizza, A., and Franceschi, C. (1996) *FEBS Lett.* **378**, 107–110
- Carmody, R. J., and Cotter, T. G. (2000) *Cell Death Differ.* **7**, 282–291
- Nylandsted, J., Rohde, M., Brand, K., Bastholm, L., Elling, F., and Jäättelä, M. (2000) *Proc. Natl. Acad. Sci. U. S. A.* **97**, 7871–7876
- Koshkin, V., and Greenberg, M. L. (2000) *Biochem. J.* **347**, 687–691
- Hoch, F. L. (1992) *Biochim. Biophys. Acta* **1113**, 71–133
- Hoch, F. L. (1998) *J. Bioenerg. Biomembr.* **30**, 511–532
- Snodderly, D. M. (1995) *Am. J. Clin. Nutr.* **62**, (suppl.) 1448–1461
- Ames, B. N., Shigenaga, M. K., and Hagen, T. M. (1995) *Biochim. Biophys. Acta* **1271**, 165–170
- Maftah, A., Ratinaud, M. H., Dumas, M., Bonte, F., Meybeck, A., and Julien, R. (1994) *Mech. Ageing Dev.* **77**, 83–96